8 Jun 87 Conference Presentation

Dynamic Stall Vortex Development and the Surface Pressure Field of a Pitching Airfoil

TA 2307-F1-38

J.A. Albertson, T.R. Troutt, W.D. Siuru,
J.M. Walker

F.J. Seiler Research Laboratory
USAF Academy CO 80840-6528

FJSRL-PR-90-0009

A detailed examination of simultaneous digitally enhanced flow visualization results and surface pressure measurements was conducted to develop insight into the relationships between dynamic stall vortex development and airfoil surface pressure levels. The experimental situation involved a two-dimensional NACA 0015 airfoil driven at constant pitching rates over attack angles from zero to 60 degrees. Specific attention was focussed on moderately low non-dimensional pitch rates such that only a single dynamic vortex was present on the airfoil surface at any one time. The analyses show that the development of a dynamic stall vortex over the top surface of the airfoil does not enhance the instantaneous lift. The initiation of the dynamic stall vortex appears to correspond closely to a leveling of the lift curve as a function of attack angle. Later rapid growth of the stall vortex accompanies a decrease in lift. The eventual detachment of the stall vortex from the airfoil corresponds to a simultaneous decrease in the pressure drag on the airfoil.

flow visualization
dynamic loads
vortices

10

UNCLASSIFIED UNCLASSIFIED UNCLASSIFIED NONE

AIAA'87

AIAA-87-1333
Dynamic Stall Vortex Development and the Surface Pressure Field of a Pitching Airfoil

J.A. Albertson, T.R. Troutt, Washington State Univ., Pullman, WA; W.D. Siuru, Univ. of Colorado, Colorado Springs, CO; and J.M. Walker, USAF Academy, Colorado Springs, CO

AIAA 19th Fluid Dynamics, Plasma Dynamics and Lasers Conference

June 8-10, 1987/Honolulu, Hawaii

Dynamic Stall Vortex Development and the Surface Pressure Field of a Pitching Airfoil

by

J.A. Albertson* and T.R. Troutt+
Washington State University

W.D. Siuru++
University of Colorado at Colorado Springs

and

J.M. Walker+
Frank J. Seiler Research Laboratory, USAF Academy

Abstract

A detailed examination of simultaneous digitally enhanced flow visualization results and surface pressure measurements was conducted to develop insight into the relationships between dynamic stall vortex development and airfoil surface pressure levels. The experimental situation involved a two-dimensional NACA 0015 airfoil driven at constant pitching rates over attack angles from zero to 60 degrees. Specific attention was focussed on moderately low nondimensional pitch rates such that only a single dynamic vortex was present on the airfoil surface at any instant in time. The analyses show that the development of a dynamic stall vortex over the top surface of the airfoil does not enhance the instantaneous lift. The initiation of the dynamic stall vortex appears to correspond closely to a leveling of the lift curve as a function of attack angle. Later rapid growth of the stall vortex is found to accompany a decrease in lift. The eventual detachment of the stall vortex from the airfoil is observed to correspond to a simultaneous decrease in the pressure drag on the airfoil.

Nomenclature

c	airfoil chord length
C_D	coefficient of pressure drag, $D/(1/2\ \rho\ U_\infty^2\ c)$
C_L	coefficient of lift, $L/(1/2\ \rho\ U_\infty^2\ c)$
p	pressure
r_o	radial distance from pivot to position on airfoil surface
s	tangential direction along airfoil surface
t	time
t^*	tU_∞/c
U_s	tangential velocity of airfoil surface
U_∞	free stream velocity magnitude
U^*	U_s/U_∞
x	free stream velocity direction
z	tangential direction on airfoil surface normal to x
α	angle of attack
$\dot{\alpha}$	attack angle rotation rate
$\ddot{\alpha}$	rate of change of rotation rate
α^+	nondimensional rotation rate $(\dot{\alpha}c/U_\infty)$
Γ	circulation density
θ	angle between chord axis and r_o
ζ	angle between local surface tangent and chord
ρ	density of air

* - Student member, AIAA
\+ - Member, AIAA
++- Associate Fellow, AIAA

Introduction

Recent experiments concerning the unsteady aerodynamics of pitching airfoils by Walker, Helin and Chou[1] and Jumper, Shreck, and Dimmick[2] have demonstrated that large percentage enhancements of maximum lift coefficients can be obtained from relatively low nondimensional pitch rates. For nondimensional pitch rates as low as $\alpha^+ = 0.05$ both experimental studies[1,2] reported increases in maximum lift coefficients of over 100% for a NACA 0015 airfoil. Even at the minimum pitch rate of $\alpha^+ = 0.02$ reported by Jumper, Shreck, and Dimmick[2] an increase of over 50% in maximum lift coefficient was observed.

These impressive experimental results demonstrate the potential benefits available from the exploitation of unsteady aerodynamic effects. However, more understanding of the connections between the complex unsteady flow phenomena and the resulting aerodynamic forces is presently needed to develop practical applications employing these effects. One of the significant practical applications involves improving the maneuverability of high performance aircraft[3]. The results presented here are aimed at improving this situation by developing direct connections between the separated flow phenomena and the instantaneous pressure forces on the airfoil.

The experimental situation analyzed in this study involves a two-dimensional NACA 0015 airfoil which is pitched at constant rotation rates from zero to 60 degrees in a uniform stream of air. Motion pictures of smoke streakline development synchronized with instantaneous surface pressure data are used to provide information concerning the relationships between the flow phenomena and the surface pressure field. Moderately low nondimensional pitch rates of $\alpha^+ = 0.1$ and 0.2 are focussed on here because under these conditions only one dynamic stall vortex is present instantaneously on the airfoil upper surface. At higher α^+ values multiple dynamic stall vortices may appear simultaneously on the airfoil upper surfaces making interpretations concerning the effects of individual dynamic stall vortices more difficult. In addition these low α^+ situations are important because, as mentioned previously, the largest changes in maximum lift coefficient for a given α^+ change are observed at these low rotation rates.

The primary focus of this study concerns the development and motion of the dynamic stall vortex and its influence on the instantaneous pressure field of the airfoil. McCroskey[4] states that the development of the dynamic stall vortex, which

apparently is a localized region of high vorticity on the upper surface of the airfoil, seems to be connected to the extension of the lift curve associated with the unsteady motion of the airfoil. To investigate this subject the present study employs image analysis techniques to quantify the growth and motion of the dynamic stall vortex for direct comparison to the resulting forces on the airfoil.

Experimental Procedures

The experiments were performed in the USAF Academy's low speed wind tunnel, which was described previously in Helin and Walker[5]. The crosssection of the test facility was 0.61 x 0.92 meters. The NACA 0015 airfoil had a chord length of 0.15 meters with a span equal to the test section dimension of 0.56 meters. For the results presented here the airfoil was pitched about the quarter chord position.

The surface pressure measurements were obtained using Endevco 8507-2 miniature pressure transducers mounted in close coupled configuration to surface pressure ports. Flow visualization streakline photographs were produced using smoke wire techniques in conjunction with high speed photography.

Digital image analysis of the photographic results were performed using an International Imaging System 570 in conjunction with a VAX 11/780 minicomputer. Analyses of the point sensor data were also carried out in digital format using the VAX 11/780 and a MassComp MC-500 microcomputer.

The results presented here are for a free stream velocity of 6.1 m/sec with pitch rates of 230 deg/sec and 460 deg/sec for the $\alpha^+ = 0.1$ and $\alpha^+ = 0.2$ cases respectively. The Reynolds number of the flow based on the airfoil chord and the free stream velocity was 63,500. Experimental observations by Walker, Helin and Chou[1] indicate that the major flow features are relatively independent of increasing Reynolds number at or beyond this value.

Results

Flow Visualization:

The development of a dynamic stall region on the NACA 0015 airfoil pitching at an $\alpha^+ = 0.2$ is shown in figure 1 through a sequence of flow visualization photographs at increasing attack angles. These photographs show that an obvious stall vortex region initially forms over the forward portion of the upper airfoil surface at an angle of attack near 25°. The dynamic vortex region then grows and develops with increasing attack angle until its final departure from the airfoil at an angle near 41°.

To define the boundary of the dynamic stall vortex for the purpose of quantifying its growth and motion a digital image analysis technique was employed which increased the contrast between light and dark areas on the photographs. The application of this technique to a typical photograph from the flow visualization depicting the flow near the upper surface of the airfoil is shown is shown in figure 2. Figure 2a shows the original image and 2b displays the resulting enhanced image. Lines drawn to indicate the boundary of the dynamic stall vortex are shown in figure 2c. The location of the outlined boundary depends upon separating the flow involved in the

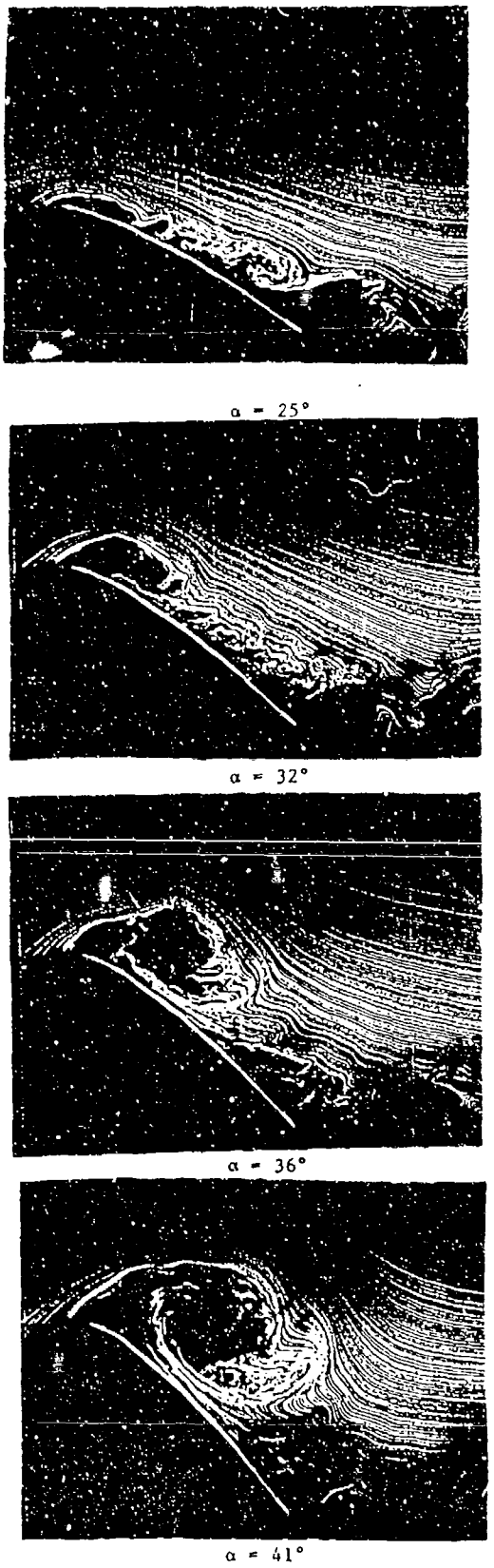

Figure 1. Sequence of flow visualization photographs at increasing attack angles, $\alpha^+ = 0.2$.

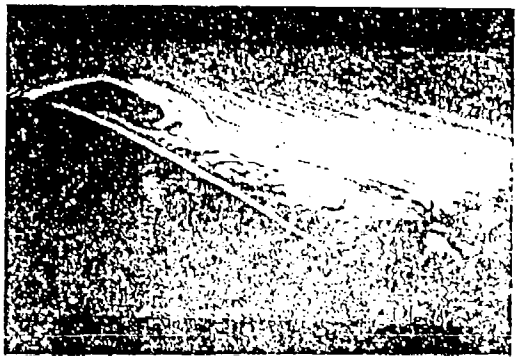

a. Original unenhanced image

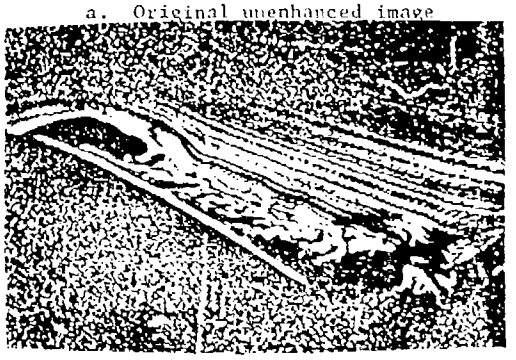

b. Image after gray level contrast enhancement.

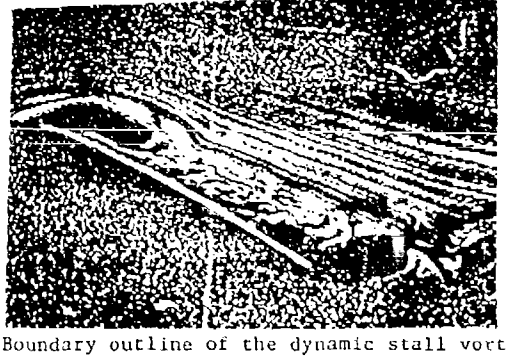

c. Boundary outline of the dynamic stall vortex.

Figure 2. Digital image analysis of visualization photographs. $\alpha = 32°$, $\alpha^+ = 0.2$.

vortex from the surrounding potential flow. This is relatively simple for the leading and upper surfaces of the stall vortex region where a clear demarcation between the chaotic turbulent rotational flow associated with the vortex region and the smooth streakline patterns associated with the outer potential flow can be made. Unfortunately, no clear separation between the downstream section of the stall vortex and the thin turbulent separated flow region covering the remaining portion of the airfoil upper surface can be determined from a single image. To delineate the aft section boundary of the stall vortex recourse is made to the eventual departure of the vortex from the airfoil surface.

A sequence of enhanced images of a typical depature event are shown in figure 3. Figure 3a shows the dynamic vortex just prior to departure. At this point no obvious separation between the lower vortex surface and the upper airfoil surface is apparent. Figure 3b displays the vortex region at approximately the moment of departure. A clear

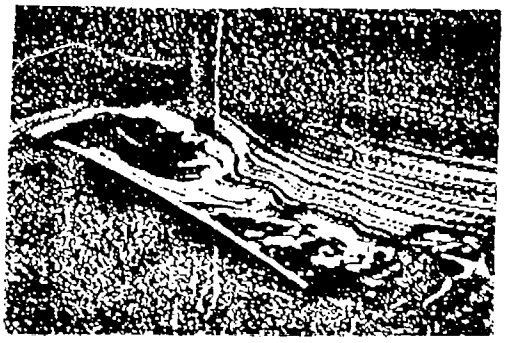

a. Vortex just prior to departure, $\alpha = 3$[illegible].

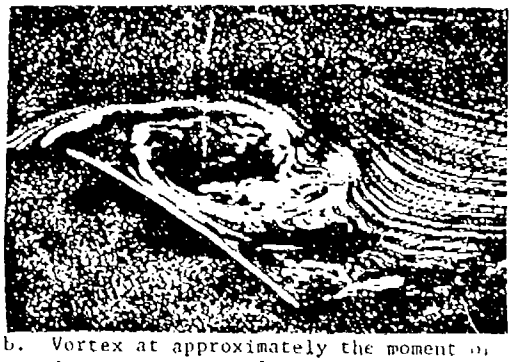

b. Vortex at approximately the moment of departure, $\alpha = 41°$.

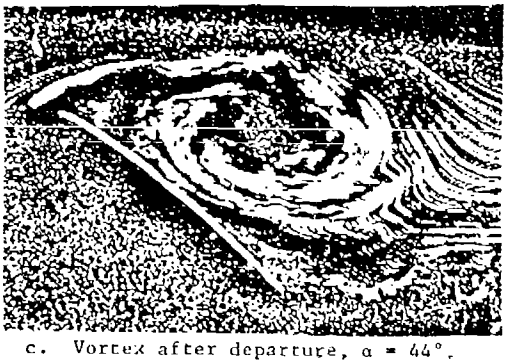

c. Vortex after departure, $\alpha = 44°$.

Figure 3. Sequence of enhanced images of dynamic stall vortex departure from the airfoil surface $\alpha^+ = 0.2$.

separation between the lower vortex boundary and the airfoil surface can be observed. Somewhat after departure the stall vortex region becomes significantly disconnected from the surface airfoil flow as indicated in figure 3c.

Once the dynamic stall vortex has departed the airfoil surface a clear distinction concerning the entire surrounding boundary of the stall vortex can be made. Working back in time frame by frame using this knowledge concerning the boundary of the departing vortex and noting similar flow features between frames a reasonably objective delineation of the downstream boundary of the stall vortex at each instant in time is possible. This approach is thus based on imposing that the bounding fluid elements associated with the stall vortex after departure be defined also as the bounding elements prior to departure. The dynamic stall vortex boundary is therefore associated with what is conventionally known as a fluid curve. Employing the previously discussed procedures the

Dynamic stall vortex size and location was quantified as a function of attack angle for direct comparison to the surface pressure measurements.

The vortex area growth as a function of attack angle was obtained using an image analysis program to color the vortex region. A 6 x 6 pixel grid was then placed over the artificially colored area. The number of grid squares associated with the colored region was then computed to produce a reasonably accurate vortex area estimate. For each α^+ value the area measurement was initiated when the dynamic stall vortex was first discernable on the top surface of the airfoil. The area measurement was then continued until the vortex became clearly detached from the airfoil surface or the maximum attack angle was reached.

Vortex growth as a function of angle of attack for constant α^+ conditions are shown in figures 4a and 4b. The farthest left point on each curve identifies the first indication of the formation of the stall vortex on the airfoil. Immediately after the initiation of the vortex both α^+ situations indicate that a region of relatively slow growth ensues suggesting a quasi-stable situation. This situation however is quickly followed by a faster growth region during which the vortex departs from the surface. The departure of the vortex from the surface occurs at 32° for the $\alpha^+ = 0.1$ case and at 41° for the $\alpha^+ = 0.2$ case.

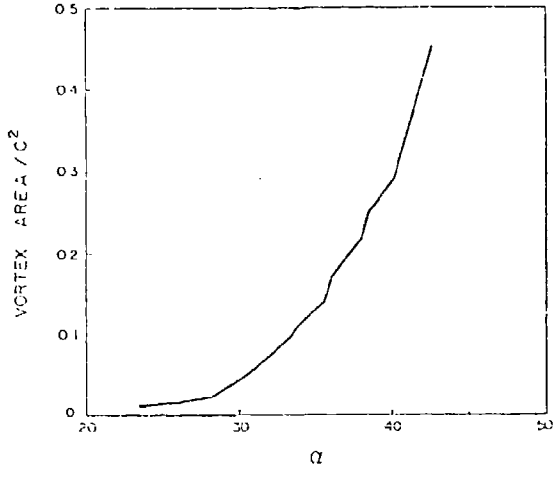

Figure 4a. Dynamic stall vortex growth as a function of attack angle, $\alpha^+ = 0.1$.

The relationship between the vortex location and the pitching motion of the airfoil was determined from measurements of the vortex center on an axis parallel to the chord. The vortex center was defined to be equidistant from the leading and trailing edges of the stall vortex at each angle of attack.

Plots of the stall vortex center location as a function of attack angle are shown in figures 5a and 5b for $\alpha^+ = 0.1$ and 0.2 respectively. The attack angle at which the stall vortex center moves to the x/c = 0.25 position coincides with the angle at which the stall vortex growth rate undergoes a rapid increase for both α^+ values of 0.1 and 0.2. This result indicates that a possi-

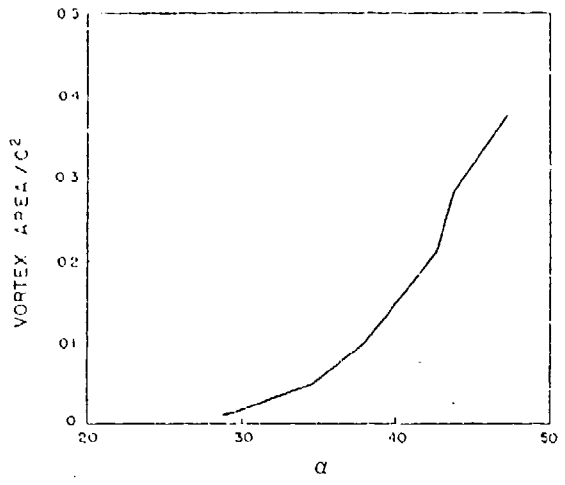

Figure 4b. Dynamic stall vortex growth as a function of attack angle, $\alpha^+ = 0.2$.

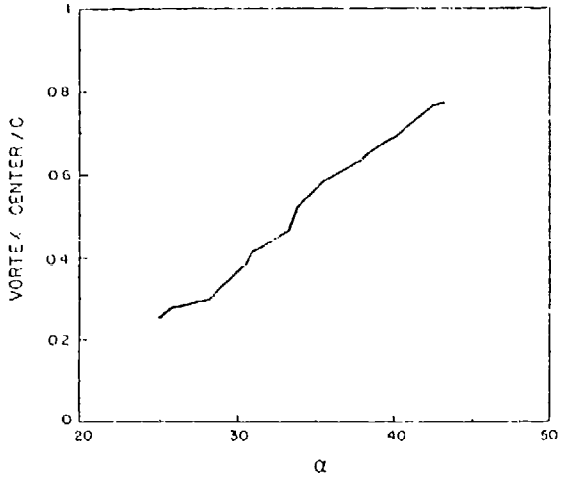

Figure 5a. Dynamic stall vortex position along the airfoil versus angle of attack, $\alpha^+ = 0.1$, U = 20 ft/sec.

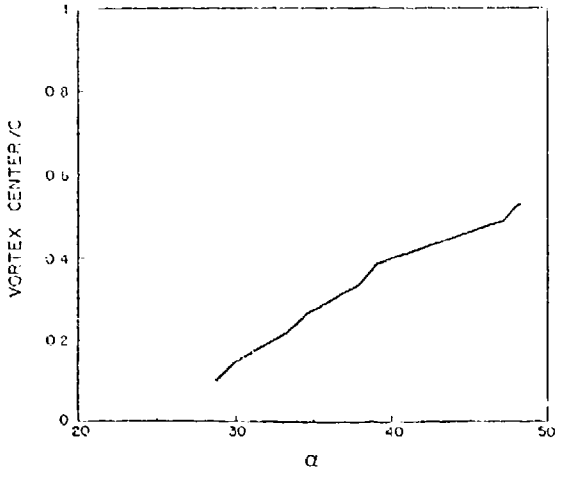

Figure 5b. Dynamic stall vortex position along the airfoil versus angle of attack, $\alpha^+ = 0.2$, U = 20 ft/sec.

ble connection between the pivot location and the dynamic stall vortex behavior may exist. Further experiments are needed to clarity this possibility.

Surface Pressure Measurements

Instantaneous upper surface pressure levels have been suggested previously by Walker et al.[1] to be apparently closely connected to the development and motion of the dynamic stall vortex. Figure 6 gives a direct comparison between the enhanced flow visualization images and instantaneous upper surface pressure levels for an $\alpha^+ = 0.2$ situation. The comparisons show that the formation of the dynamic stall vortex on the forward section of the airfoil upper surface at an attack angle of approximately 25° corresponds closely to the location of a compact area of high magnitude negative pressure. This area of low pressure apparently moves with the stall vortex as indicated in the $\alpha = 30°$ view and becomes less intense as the stall vortex grows and eventually departs from the airfoil at an angle of attack near 40°. Both the upper surface pressure levels and the surface pressure gradient are shown in the graphs. The surface pressure gradient curves are especially useful for determining the motion of the dynamic stall vortex in association with the movement of the large peak in the pressure gradient.

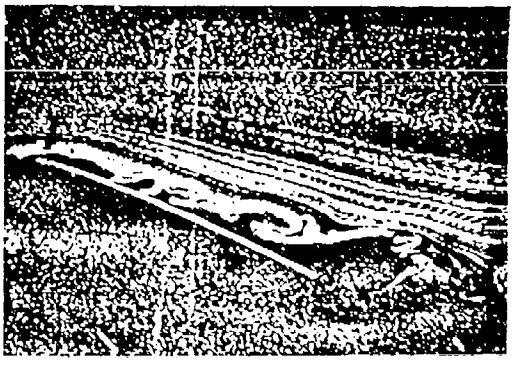

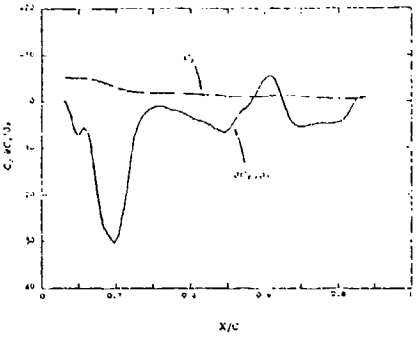

Figure 6a. Comparison between enhanced image and upper surface pressure distributions, $\alpha = 25°$.

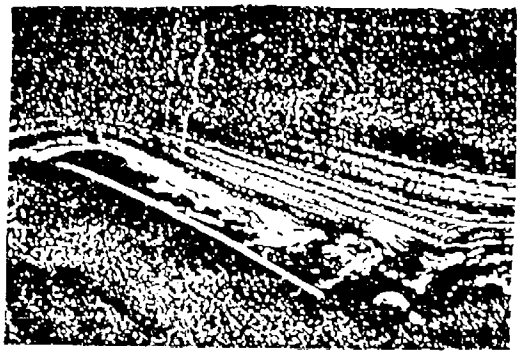

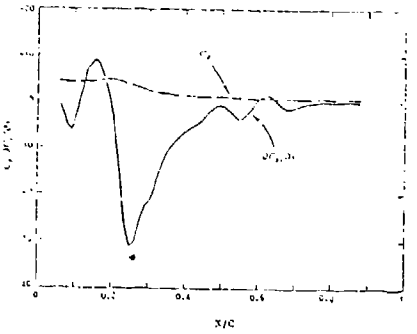

Figure 6b. Comparison between enhanced image and upper surface pressure distributions, $\alpha = 30°$.

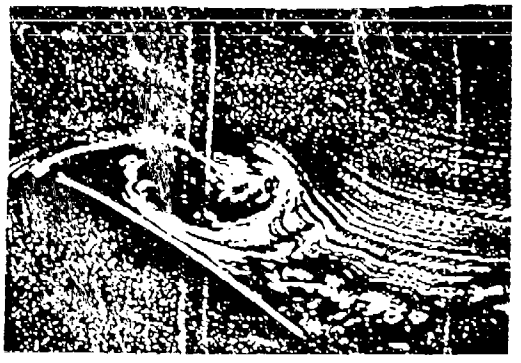

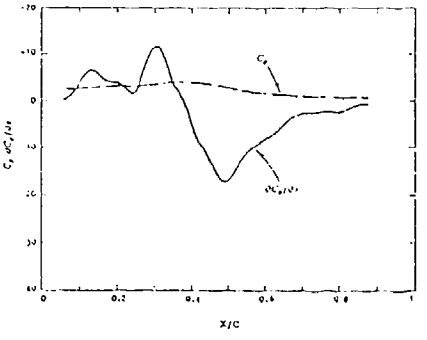

Figure 6c. Comparison between enhanced image and upper surface pressure distributions, $\alpha = 40°$.

Figure 7 shows lift coefficients obtained from both upper and lower surface pressure measurements as a function of α for an $\alpha^+ = 0.2$. The lift coefficient curves indicate that a general reduction in slope occurs near an attack angle of 24° which corresponds closely to the observation of the vortex initiation angle mentioned previously. The curve acquires a negative slope near an attack angle of 38° which corresponds closely to the beginning of the fast vortex growth region previously discussed.

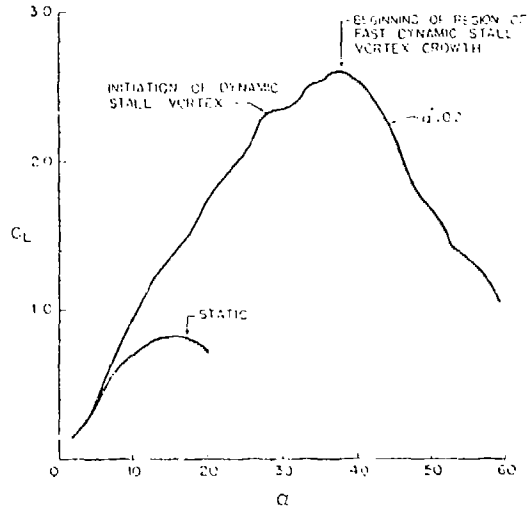

Figure 7. Lift coefficient as a function of attack angle for static and dynamic airfoil pitching motion, $\alpha^+ = 0.2$.

Figure 8 displays the experimentally measured pressure drag coefficient as a function of α for an $\alpha^+ = 0.2$. The drag coefficient increases up to approximately 45° and then begins a steady decrease. The beginning of this decrease in drag level appears to correspond closely to the angle of detachment of the stall vortex from the airfoil surface observed previously.

Analysis of Vorticity Generation

To explain the large changes in maximum lift coefficient experienced by the airfoil at these relatively low pitching rates an analysis of vorticity generation from the airfoil surface needs to be developed. In a recent work Morton[6] has shown that the vorticity generation in a homogeneous fluid may only take place at rigid boundaries and that the generating mechanisms are the tangential surface pressure gradient and the tangential surface acceleration of the boundary. This deduction can be mathematically represented by the equation

$$\frac{d\Gamma_z}{dt} = \rho^{-1} \left.\frac{\partial p}{\partial s}\right|_o + \frac{dU_s}{dt} \qquad (1)$$

where $d\Gamma_z/dt$ is the flux of z direction vorticity from the surface fluid density, $\partial p/\partial s\ _o$ is the tangential pressure gradient along the rigid surface in a direction normal to the z axis, and dU_s/dt is the tangential acceleration in the s direction of the rigid surface. This equation

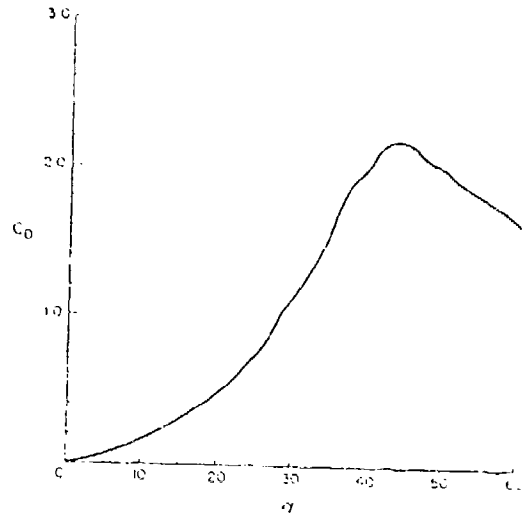

Figure 8. Pressure drag coefficient as a function of attack angle, $\alpha^+ = 0.2$.

explicitly separates the effects of the fluid dynamics through the pressure gradient from the effects of the rigid surface acceleration on the vorticity generation rate at the surface. Although the surface pressure gradient is dependent upon the flow and cannot easily be obtained for turbulent flows, except from experiments, the surface acceleration term can be easily calculated for specific experimental situations.

For the case of an airfoil pitching about a fixed pivot the surface acceleration term can be given by the following relation

$$\frac{dU_s}{dt} = r_o \left[\dot{\alpha}^2 \cos(\theta + \xi) + \ddot{\alpha} \sin(\theta + \xi)\right] \qquad (2)$$

For the specific airfoil experiments evaluated thus far, $\dot{\alpha}$ was maintained constant during the measurements so equation (2) reduces simply to

$$\frac{dU_s}{dt} = r_o \dot{\alpha}^2 \cos(\theta + \xi) \qquad (3)$$

The surface acceleration term for a specific airfoil geometry pitching about at a fixed pivot at a constant rotation rate is thus solely dependent on $\dot{\alpha}^2$. Competition between the pressure gradient term and the surface acceleration term with respect to vorticity generation for constant density flow can therefore be scaled by $\dot{\alpha}^2 c^2/U_\infty^2$ or $\dot{\alpha} c/U_\infty$. This nondimensional parameter has in fact been noted previously by Walker, Helin, and Chou[1] as a primary controlling factor in their pitching airfoil experiments. This parameter was assigned the symbol α^+ by Walker, Helin, and Chou[1].

Figure 9 shows the computed values of the vorticity flux density from the top surface of a NACA 0015 airfoil as a function of chord position for various values of the parameter α^+. For these curves the hinge position was located on the airfoil chord at 0.25 c from the leading edge. The results show that both positive and negative vorticity is produced by the top surface of the

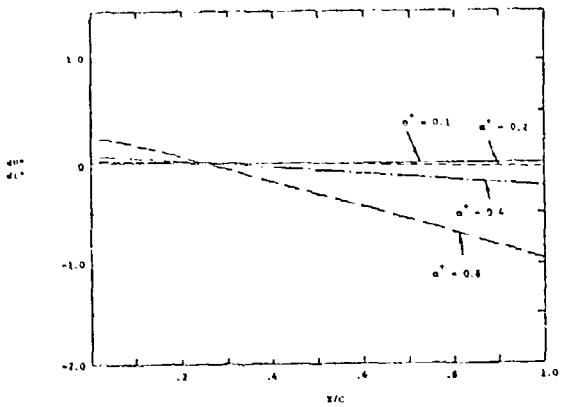

Figure 9. Tangential surface acceleration curves for pitching airfoil at various α^+ values with pivot at $x_h = 0.25$.

airfoil with a zero vorticity flux located approximately at the hinge location because the sum of the two angles $(\theta + \xi)$ goes through 90° in this vicinity. Since the NACA 0015 is a symmetric airfoil the bottom surface vorticity production is a negative of the top surface generation rate, and the total instantaneous vorticity generation produced by the tangential surface acceleration of the pitching airfoil will be identically zero at all times. In addition one can also conclude from Morton's[6] discussion that the total vorticity production from the tangential surface pressure gradient will also identically cancel at all times such that no net vorticity is created by the body.

The determination of the vorticity generation by the tangential surface pressure gradients is considerably more complex than the surface acceleration analysis since the surface pressure gradient depends directly on the flow character. To evaluate this generation term point surface pressure measurements from the experimental results were analyzed.

Typical surface pressure results are shown for a value of $\alpha^+ = 0.2$ at various attack angles below 20° in figure 10. The surface pressure gradients at all angles of attack are positive over most of the airfoil top surface. According to equation (1) these positive gradients will produce positive z direction vorticity. This positive vorticity production will tend to induce reversed or separated flow close to the airfoil. This is, of course, the situation that arises in steady aerodynamics as the attack angle nears the stall angle, and the separation region spreads over the airfoil surface. For pitching airfoils this result is avoided by apparently inhibiting the spread of the separation region over the upper airfoil surface.

A comparison of the two vorticity generation terms can now be made. The negative z vorticity produced by the surface acceleration term downstream of the pivot location will tend to counteract the positive vorticity produced by the surface pressure gradients. However, for cases involving relatively low α^+ values (0.1 - 0.4) it would not appear that the surface acceleration values are of comparable magnitude to the levels of pressure gradient encountered even at moderately low angles of attack. The large influence of the airfoil pitching motion on the maximum coefficient of lift observed by Walker et al.[1] and Jumper et al.[2]

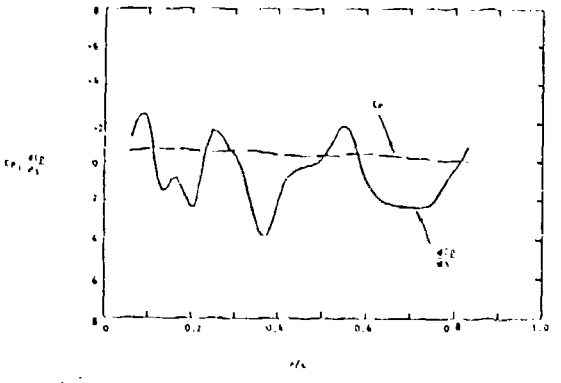

Figure 10a. Instantaneous upper surface pressure coefficient and gradient, $\alpha = 0$, $\alpha^+ = 0.2$.

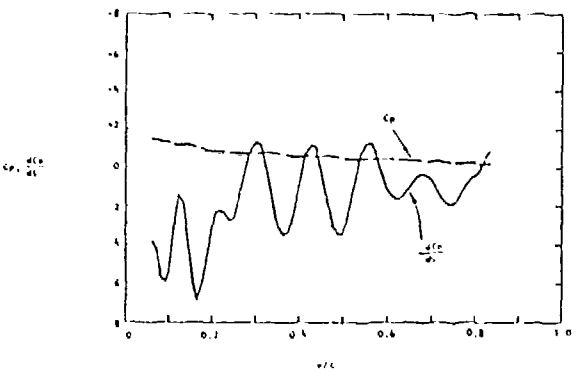

Figure 10b. $\alpha = 10°$, $\alpha^+ = 0.2$.

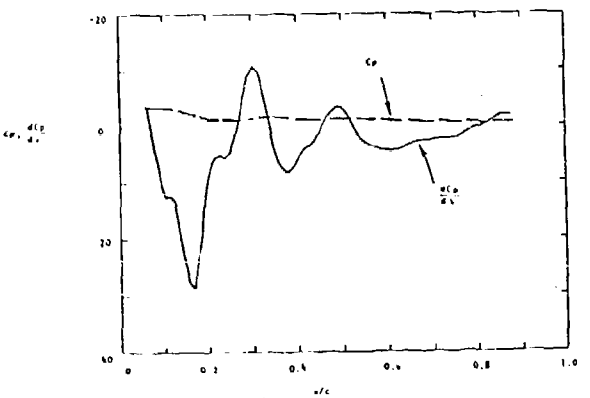

Figure 10c. $\alpha = 20°$, $\alpha^+ = 0.2$.

can thus apparently not be explained easily through a simple superposition of vorticity generation terms. Since the surface pressure gradient term is a consequence of the fluid dynamics of the system, small changes in the boundary conditions must be reflected as large effects in the flow through the nonlinearity of the high Reynolds number flow processes.

Conclusions

The results of this study indicate that the development of the dynamic stall vortex on a pitching airfoil corresponds closely to a leveling

of the lift curve as a function of attack angle. The later fast growth of the stall vortex is indicated as corresponding to a reduction in the lift curve with increasing attack angle. In addition it was observed that a general decrease in pressure drag was associated with the departure of the stall vortex from the airfoil surface. These findings indicate that the development and growth of the dynamic stall vortex can be associated with the loss of vorticity from the boundary layer of the airfoil with a consequent loss in lift. The dynamic stall vortex thus appears to be largely a consequence of the unsteady airfoil motion and not a fundamental generation mechanism for producing the enhanced lift. Since much of the enhanced lift of the airfoil occurs prior to the initiation of the dynamic vortex, it would appear that the unsteady motion of the airfoil itself is primarily responsible for the large enhancements in observed lift.

Based on these previous observations the vorticity production by the unsteady airfoil motion should be of considerable importance for understanding the large changes in near surface flow character. Investigation of the vorticity production by the unsteady surface motion and the instantaneous surface pressure gradient terms indicated that the α^+ parameter should be related to the relative strengths of these two terms for constant pitch rate motions. This result supports experimental findings which had also found that α^+ was a controlling nondimensional parameter for constant pitch rate situations.

Acknowledgements

"Research sponsored by the Air Force Office of Scientific Research/AFSC, United States Air Force, under Contract F49620-85-C-0013. The United States Government is authorized to reproduce and distribute reprints for governmental purposes notwithstanding any copyright notation herein."

References

(1) Walker, J., Helin, H., and Chou, D., "Unsteady Surface Pressure Measurements on a Pitching Airfoil," AIAA Paper 85-0532, AIAA Shear Flow Control Conference, Boulder, CO, March 1986.

(2) Jumper, E.J., Shreck, S.J. and Dimmick, R.L., "Lift-Curve Characteristics for an Airfoil Pitching at Constant Rate," AIAA Paper 86-0117, The Aerospace Sciences Conference, Reno, NV, January 1986.

(3) Herbst, W.B., "Supermaneuverability," Proceedings from Workshop on Unsteady Separated Flows, USAFA, Department of Aeronautical Engineering, University of Colorado, Boulder, CO, August 1983, 1-9.

(4) McCroskey, W.J., "Unsteady Airfoils," Ann. Rev. Fluid Mech., 14, 1982, 285-311.

(5) Helin, H.E., and Walker, J.M., "Interrelated Effects of Pitch Rate and Pivot Point on Airfoil Dynamic Stall," AIAA Paper 85-0130, 1985.

(6) Morton, B.R., "The Generation and Decay of Vorticity," Geophys. Astrophy. Fluid Dynamics, 28, 1984, 277-308.